Journal of ELECTRONIC MATERIALS, Vol. 46, No. 4, 2017
DOI: 10.1007/s11664-016-5273-z

Nanostructure $ZnFe_2O_4$ with *Bacillus subtilis* for Detection of LPG at Low Temperature

SOLLETI GOUTHAM,[1] DEVARAI SANTHOSH KUMAR,[2] KISHOR KUMAR SADASIVUNI,[3] JOHN-JOHN CABIBIHAN,[3] and KALAGADDA VENKATESWARA RAO[1,4]

1.—Centre for Nano Science and Technology, Jawaharlal Nehru Technological University Hyderabad, Kukatpally 500085, Telangana State, India. 2.—Department of Chemical Engineering, Indian Institute of Technology, Hyderabad, Kandi, Sangareddy 502285, Telangana State, India. 3.—Department of Mechanical and Industrial Engineering, Qatar University, P. O. Box 2713, Doha, Qatar. 4.—e-mail: kalagadda2003@jntuh.ac.in

The present study deals with the development of a chemical sensor for the detection of liquefied petroleum gas (LPG) at a low operating temperature using Zinc ferrite ($ZnFe_2O_4$)/*Bacillus subtilis* (*B. subtilis*) hybrid nanostructures. The nanostructure $ZnFe_2O_4$ and *B. subtilis* powder, taken in equal proportion was made into films using the spin coating technique. X-ray diffraction, thermal analysis, scanning electron microscopy, and transmission electron microscopy were used to study morphology, structure and crystallite size. The sensing properties of the hybrid structure were studied and excellent response was observed in the temperature range of 50–55°C for 400 ppm LPG, when compared to the individual components of the hybrid. The signal output of the proposed sensor were extremely stable for more than 30 days. This method proposes the usage of the biomolecule/metal oxide composites in electronics and helps to reduce the metal oxide usage.

Key words: Hybrid-nanostructures, $ZnFe_2O_4$, *Bacillus subtilis*, chemical sensor, liquefied petroleum gas

INTRODUCTION

In the current scenario, it is difficult to find a reliable, low temperature friendly and accurate detector to sense gas leakage. To detect and control the release of explosive and toxic gases in the environment, accurate and selective solid-state sensors are necessary, instead of the less efficient improper detectors.[1–3] Liquefied petroleum gas (LPG) is a very commonly used gas fuel for both domestic and industrial purposes. LPG is an odorless and colorless gas which makes its detection a major task for domestic purposes, and it is achieved by adding ethyl mercaptan, which gives an odor to LPG that helps in its detection. But for industrial purposes, where large quantities are used, this might be a difficult task. Gas sensor materials with precise electrical properties and better sensitivity at low cost is difficult to obtain, causing its increasing demand. Reports have come out on sensors based on metal oxides; however, they possess certain limitations. While a few sensors working at low temperature are not able to detect low level LPG,[4–7] a few others with good sensitivity show least durability. This points towards the fact that either sensitivity or operating temperature must be compromised while designing sensors. Wang et al.[8] reported that sensors, with supreme sensitivity working at high operating temperature, cause an increase in the power consumption. It has been recently known that a certain amount of microbial powder consisting of peptidoglycan biomolecules, which are present on nucleic acids and proteins, have a novel semiconducting functional nature which can be used as a substitute for the conventional materials.[9] In this regards, *B. subtilis* proteins are sources of biological materials, which are well-suited for

(Received July 31, 2016; accepted December 29, 2016; published online January 18, 2017)

different applications.[10] Microbial *B. subtilis* is a gram positive rod shaped structure, which is abundantly available with biodiversity. The biggest advantage of organic electronics like organic sensors and organic displays is that these devices are flexible, lightweight and can also be fabricated in large areas compared to the conventional materials. Xi et al.[11] reported that the *Bacillus* spores are being used in biomedical devices, sensors, robotics and also in energy harvesting. *B. subtilis* protein molecules are excited, and the electrons transmit fast due to the tunneling effect.[12] Due to this reason, bacterial proteins transmit electrons in picosecond.[13] Ferrites are significant materials in terms of electrical properties and their electrical resistivity changes when the gas molecules get adsorbed to them. In addition, depending on the surface area of a particular material, the gas sensing rate varies.[14] The addition of zinc ferrites is done as it is a functional inorganic sensing materials, which is much used in chemical catalysts and electronic devices. Presently, the nanostructure $ZnFe_2O_4$ has also received special attention for its gas sensing feature. $ZnFe_2O_4$ acts as a saturation magnetization factor with high electrical resistance and good chemical stability. Electrical conductivity is one of the most important properties of nanostructure $ZnFe_2O_4$ that gives valuable information about conduction mechanisms compared to other metal oxides.[15,16] These nanostructures have a large surface area, which helps them in having the highest sensitivity towards gas leakage.[17]

In the present work, a new sensing material is introduced with high sensitivity and low operating temperature to detect LPG leakage. Studies were performed on samples made by mixing nanostructured Zinc ferrite ($ZnFe_2O_4$) with *Bacillus subtilis* (*B. subtilis*, acting as a semiconductor) powder in equal proportions. The mechanism of sensing at various temperatures is investigated and correlated with the structural and electrical properties.

EXPERIMENTAL PROCEDURE

Methodology

Nanostructured $ZnFe_2O_4$ was synthesized using the sol-gel auto combustion method.[18] Though different methods such as laser ablation, chemical vapor deposition, high energy milling and sol-gel auto combustion are available, the auto combustion method involving an exothermic reaction between a fuel and metal nitrate is the simplest. Glycine was used as the fuel and iron and zinc nitrate as metal nitrates along with deionized water as the solvent. Iron nitrate $(FeNO_3)_3{\cdot}9H_2O$ and Zinc nitrate $(ZnNO_3)_2{\cdot}6H_2O$ of 99% purity were purchased from Sigma Aldrich USA. Metal nitrate/fuel stoichiometry was calculated based on propellant chemistry.[19] The metal nitrates and fuel were dissolved in a minimum amount of distilled water and were thoroughly stirred by magnetic stirring until a clear solution was formed and then further heated to 100°C under continued stirring. Further annealing was performed at 650°C for 4 h in order to attain the final product.

The synthesized nanostructured $ZnFe_2O_4$ was investigated for crystal phase composition using x-ray diffraction studies by a Bruker D8 Advanced and *CuKα* radiation source $\lambda = 0.154$ nm. Particle size and structure was analyzed by a transmission electron microscope (TEM Philips, Holland instrument) operating at an accelerating voltage of 120 kV. Morphological studies were carried out by scanning electron microscopy using Hitachi S-3400 N, Japanese model. Thermal analysis (TG/DTA) technique to measure the weight loss in a material was done as a function of temperature and time using S-II EXSTAR-6000.

Preparation of *B. subtilis* Powder

Bacillus subtilis isolated from the soil was used as a source material. One loop of diluted soil sample was streaked on nutrient agar plate which was kept in a sterile condition. The plate was incubated for 24 h at 37°C temperature until white colored colonies were obtained. These synthesized cultures showed positive results for biochemical tests indicating the presence of *B. subtilis* in the plates. The culture was sub-cultured to obtain more colonies of *B. subtilis* Fig. 1a and b. Cells were centrifuged and supernatant was discarded. The obtained biomass pellets were converted to powder and were allowed to overnight dry. The obtained powder's protein estimation was done by the Bradford assay, which was found to be ~9.16 μg/ml. The prepared protein was mixed with synthesized nanomaterial to obtain hybrid composites. After adding protein to the nanomaterial, a final concentration of protein is maintained at ~8.92 μg/ml.[20]

Design of Experimental Set-Up to Study Sensing Performance

An in-house gas sensing setup unit was used to measure relative resistance change, response and recovery time of the sensor. The whole setup was placed in a vacuum chamber with a temperature controller. A constant flow rate of desired gas by mass flow controllers (Aalborg, USA), a heater with ±1°C, and silver contacts were used for monitoring and measuring electrical parameters of the sensor using a Keithley 2750 multimeter. A thermocouple was connected to the setup, to measure temperature inside the chamber.

The sensor sample was placed over a heating coil for 5 min to create atmospheric pressure. The resistance change, recovery time and saturation time of sensor depending upon the operating temperature, concentration of an analyte, sensing material and electrode model, etc.[21] were checked. Relative resistance (A_R) was calculated using the $(R_a - R_g)/R_a$ equation.[22] The resistance that was

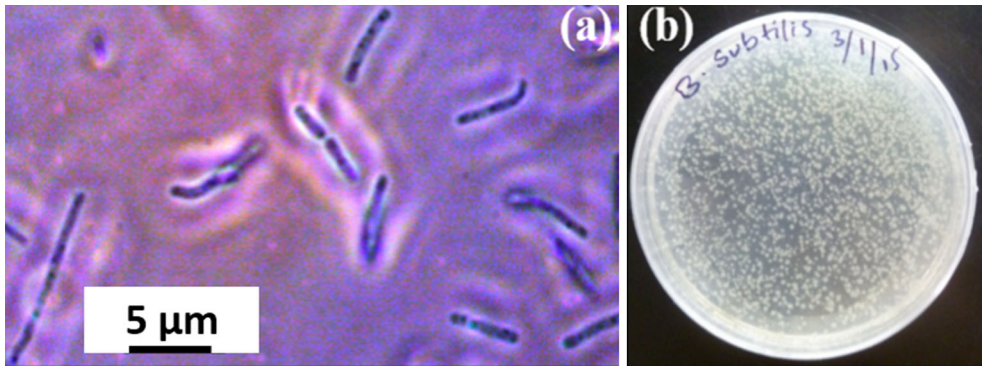

Fig. 1. (a) Microscopic image of rod shaped *B. subtilis* at 5 μm magnification and (b) Colonies of *B. subtilis* on an agar plate.

measured at the atmospheric pressure and under the flow of synthetic air flow was denoted as $R_{air,}$ and the resistance measured at atmospheric pressure and under the flow of LPG was denoted as R_{gas}.

RESULTS AND DISCUSSION

Characterization

The XRD patterns of prepared samples showing well-resolved peaks are depicted in Fig. 2a. XRD confirms the face-center and cubic structures in the prepared material, and the pattern is recorded over a range of 2θ angles from 20° to 80°. The 2θ of nanostructured $ZnFe_2O_4$ is obtained at 29.9, 35.2, 42.8, 53.1, 56.6 and 62.2 corresponding to the planes (220), (311), (400), (422), (511) and (440) and provides clear evidence for the formation of spinel type cubic structure of the ferrite. These results are well matched with JCPDS (file no 89-1012). According to JCPDS, the volume of the unit cell for the ferrite is 599.72. The crystallite size was calculated using Scherrer's formula[23] i.e.,

$$D = 0.9\lambda/\beta\cos\theta,$$

where, D is the average crystallite size (nm), λ the wavelength of x-rays, θ the diffraction angle and β, the full width at half maximum in radians. Using the above equation the average crystalline size was obtained as 33.6 nm.

The SEM images of the prepared nanostructures $ZnFe_2O_4$ are shown in Fig. 2b and c. The image shows the presence of particles that are agglomerated in nature. A close inspection reveals the presence of porous network structure between the particles. This nanostructure $ZnFe_2O_4$ shows high porosity as expected because of the increased fuel-to-oxidizer ratio.[24] The distribution of particles and size of particles were analyzed by TEM as shown in Fig. 2d. The TEM image further confirms the porous nature of the obtained nanostructures and coagulated zinc particles with ferrite particles. The particles are uniform and the average particles size is 100 nm. The particle size obtained from TEM and XRD has a very good agreement.

The thermal properties of the nanostructure $ZnFe_2O_4$ synthesized via the sol–gel auto-combustion route was characterized by TG–DTA during the temperature range from 0°C to 800°C shown in Fig. 3. The weight loss of $ZnFe_2O_4$ in the first stage, below 100°C, is attributed to the loss of adsorbed water on the surface of the material. The second stage around 120–350°C is due to the release of residual chemisorbed water and the release of organic residues. The third stage appeared after temperature 350°C is ascribed to the removal of hydroxyl group on the materials. We also obtain similar thermal properties for the composite. The protein does not show any significant change in the thermal property of $ZnFe_2O_4$.

LPG Sensing Performance

Fabrication of Device and LPG Sensing Analysis

A Si substrate cleaned with solvents—acetone, ethanol, chromic acid and distilled water—by ultrasonication was used for sample deposition. The sensing film fabricated with nanostructured $ZnFe_2O_4$ and bacterial powder in equal proportions was coated on 1 μm thick SiO_2 layered Si substrate, using a spin coater at 3000 rpm for 60 s.[25] Silver contacts were made on two ends of the sensing film in order to get two-end electrode configuration. The schematic representation of the gas sensing device is illustrated in the inset of Fig. 4a. Figure 4a shows the current–voltage (I–V) characteristics of $ZnFe_2O_4$ and $ZnFe_2O_4$/*Bacillus subtilis* composite arrays. These curves show significant difference in both forward and reverse directions. It is clear from the figure that, a non-linear variation of current with gate voltage is observed for both films. The composite has a p–n junction property observed from the current asymmetry under both bias (forward and reverse) directions. This property explains that, between the *Bacillus subtilis* and $ZnFe_2O_4$ nanoparticles, a heterojunction might have been established. The gas sensing application of the pure nanostructured $ZnFe_2O_4$, *B. subtilis* powder, and $ZnFe_2O_4$/*B. subtilis* hybrid nanostructures were tested for LPG at 400 ppm. The sensing film

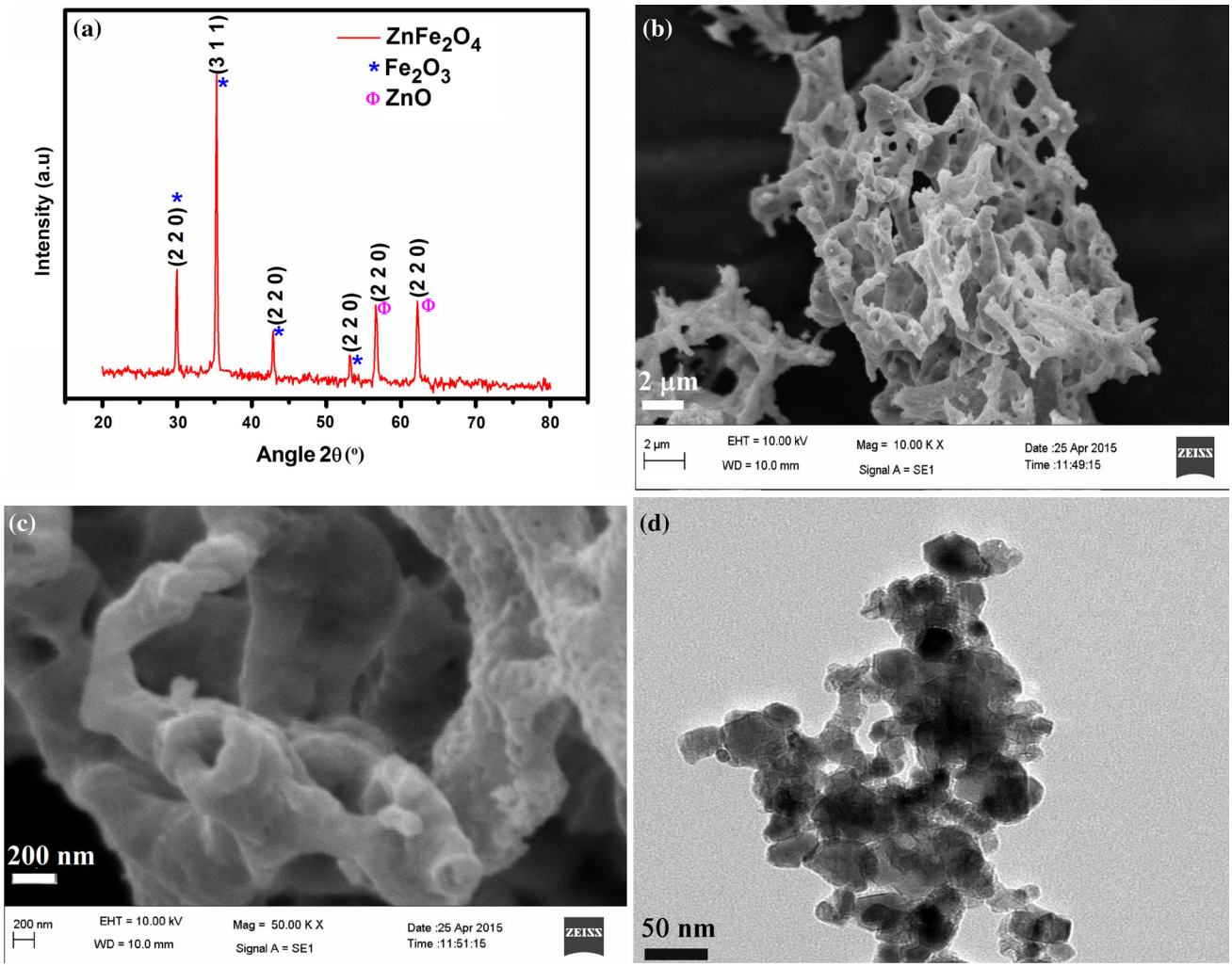

Fig. 2. (a) X-ray diffraction pattern of nanostructure $ZnFe_2O_4$ (b and c) Scanning electron microscopy images shows nanostructure $ZnFe_2O_4$ at room temperature and (d) Transmission electron microscopy micrograph of nanostructure $ZnFe_2O_4$.

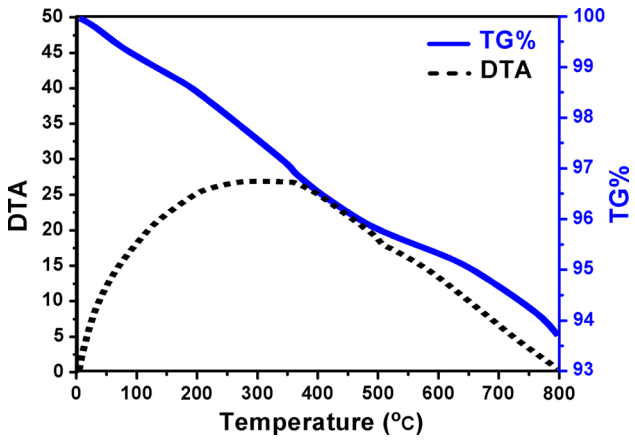

Fig. 3. TG/DTA analysis of nanostructure $ZnFe_2O_4$ curve.

responses are expressed as relative resistance change (A_R) at a controlled flow rate for the samples in the temperature range 30–325°C for $ZnFe_2O_4$, 20–100°C for $ZnFe_2O_4$/*B. subtilis* hybrid nanostructures and *B. subtilis* powder. As shown in the Fig. 4b, LPG sensing properties strongly depend on the operating temperature, which mainly maintains the activation process. In general, temperature initiates the chemical reaction taking place on the particle surface and speeds up the diffusion of the gas molecule to the sensor surface.

The sensor response was measured by a multimeter with a fixed bias voltage of 2 V. The results indicate that $ZnFe_2O_4$/*B. subtilis* hybrid nanostructures and $ZnFe_2O_4$ show almost similar sensitivity at various operating temperature with constant LPG level (400 ppm). In the case of *B. subtilis* powder, low sensitivity was observed due to lack of a sensing element. With increase in operating temperature, the sensitivity increased initially to a maximum of 33.28% and then decreased by further temperature increment for $ZnFe_2O_4$. Rathore et al.[26] observed a similar type of behavior with $NiZnFe_2O_4$, which showed around 34% of sensitivity

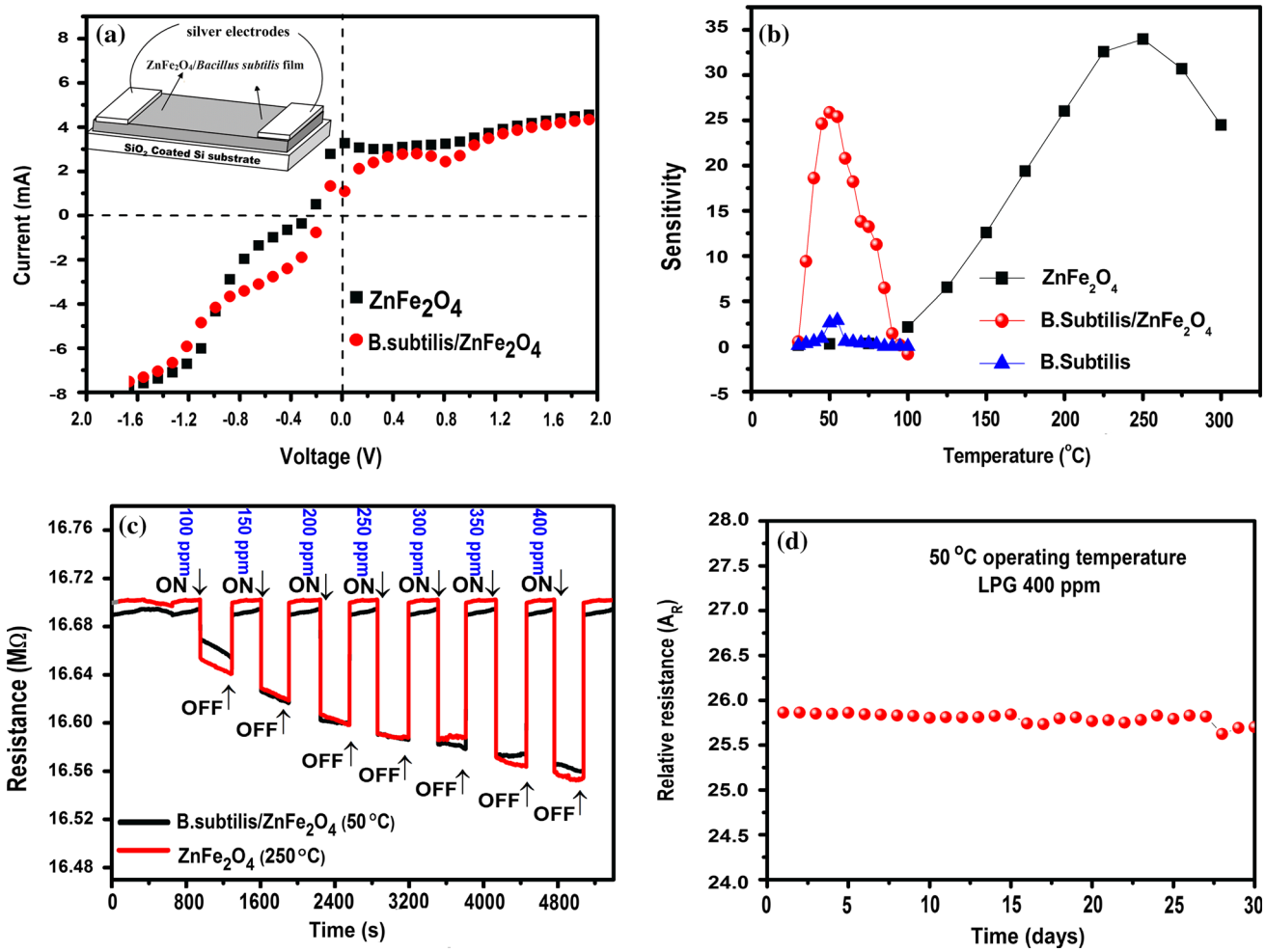

Fig. 4. (a) *I–V* curve of $ZnFe_2O_4$ and $ZnFe_2O_4$/*B. subtilis*. (Inset is a simplified illustration of the chemiresistive gas sensor) (b) Sensitivity for $ZnFe_2O_4$, *B. subtilis* with $ZnFe_2O_4$ and pure *B. subtilis* powder (c) Dynamic characteristics of $ZnFe_2O_4$ and $ZnFe_2O_4$/*B. subtilis* sensors resistance with respect to time at 400 ppm of LPG and (d) Durability of *B. subtilis* with $ZnFe_2O4$ at 400 ppm of LPG sensing.

at 300°C operating temperature. $ZnFe_2O_4$/*B. subtilis* hybrid sensors have reached the maximum sensitivity at normal operating temperature at 50°C, because of high conversion of adsorbed oxygen species, and thus attract more electrons from the nanomaterial. The sensing mechanism for LPG detection by zinc ferrite ($ZnFe_2O_4$)/*B. subtilis* hybrid nanostructures were explained based on adsorption–desorption kinetics and oxidation–reduction of gas molecules on the surface, which modulates the conductivity of the sensor. The LPG contains a mixture of gas and methane, propane and butane; etc., that are the main constituents, where propane and butane dominate.[27] The possibility of chemisorbed oxygen molecules in the form of O^{2-}, O^- or O_2^{2-} is known and the formation of oxygen ions depends on the operating temperature. The modulation of electrical conductivity of the sample is due to the electron depletion from the surface of these materials.[28] The basic principle behind high sensitivity is the formation of a heterojunction barrier. The interaction of LPG molecules at the heterojunction interface of $ZnFe_2O_4$/*B. subtilis* results in the reduction of carrier concentration near the interface. The potential barrier of the heterojunction interface was enhanced by a decrease in carrier concentration.[29] The enhanced electron transport in $ZnFe_2O_4$/*B. subtilis* hybrid might be due to high protein content and high current density during the interaction between the oxygen and analytic gas molecules, thus $ZnFe_2O_4$/*B. subtilis* hybrid nanostructures had shown an excellent sensitivity at a normal operating temperature of 50°C.

The dynamic sensitivity with respect to time at a stable concentration of LPG for nanostructured $ZnFe_2O_4$ and $ZnFe_2O_4$/*B. subtilis* hybrid sensors was performed and is shown in Fig. 4c. The sensitivity time for both the sensors seems to be equal. It was observed that, pure nanostructure $ZnFe_2O_4$ sensor, the highest sensitivity was reached in 751.8 s and for $ZnFe_2O_4$/*B. subtilis* hybrid nanostructures it took 840 s. Nanostructured $ZnFe_2O_4$ was uniformly mixed with the bacterial powder to

form hybrid nanostructures possessing electrical interaction between the charged surface structure of the bacterial powder and the porous $ZnFe_2O_4$ nanomaterial ions. In this case, a bacterium composed of thick multilayered peptidoglycans can contribute to high surface charge, which helps to improve sensing at normal temperature. Finally, the results indicated that the LPG detection limit of $ZnFe_2O_4$/*B. subtilis* is 100 ppm at 50°C. Shim et al.[30] used *B. subtilis* as a highly reversible lithium storage in rechargeable Li-ion batteries, and these bacteria can be used for several technological applications like sensors, actuators, and supercapacitors.

CONCLUSION

We demonstrated a low temperature gas sensor based on $ZnFe_2O_4$/*B. subtilis* hybrid nanostructures working at low temperatures. The XRD and Bradford method was used to evaluate the crystallinity and protein concentration in the sample. The sensing experiments concluded that proteins will enhance the sensitivity at low temperature compared to sensors without proteins. The proposed hybrid sensor showed excellent stability for 30 days with a constant temperature at 400 ppm of LPG, and further it showed an excellent sensitivity at lower operating temperatures. These hybrid materials can be used as leakage detectors in various industries, gas cars, domestic areas, hotels, and factories.

ACKNOWLEDGEMENTS

The author KVR is thankful to the Science and Engineering Research Board—Department of Science and Technology [Project No. SB/EMEQ-183/2013] for generous financial support. The first author would also like to extend his sincere gratitude to KVR, KKS and DSK for their unconditional support and encouragement.

REFERENCES

1. N. Yamnzoe and N. Miura, *IEEE Trans. Compon. Packag. Manuf. Technol.* 18, 252 (1996).
2. C. Pijolat, C. Pupier, M. Sauvan, G. Tournier, and R. Lalauze, *Sens. Actuators, B* 59, 195 (1999).
3. J.S.G.D. Santas-Alves and R.F. Patier, *Sens. Actuators, B* 59, 69 (1999).
4. C.C. Wang, A.A. Akbar, and M.J. Madou, *J. Electroceram.* 2, 273 (1998).
5. V.R. Shinde, T.P. Gujar, and C.D. Lokhande, *Sens. Actuators, B* 120, 551 (2007).
6. L. Satyanarayana, C.V. Gopal Reddy, S.V. Manorama, and V.J. Rao, *Sens. Actuators, B* 46, 1 (1998).
7. B.-J. Kim, I.-G. Song, and J.-S. Kim, *Electron. Mater. Lett.* 10, 509 (2014).
8. C.L. Wang, W.S. Hwang, K.M. Chang, H.H. Ko, C.S. His, H.H. Huang, and M.C. Wang, *Int. J. Mol. Sci.* 12, 935 (2011).
9. B. Munge, S.K. Das, R. Ilagan, Z. Pendon, J. Yang, H.A. Frank, and J.F. Rusling, *J. Am. Chem. Soc.* 125, 12457 (2003).
10. M.T. Giardi and E. Pace, *Trends Biotechnol.* 23, 257 (2005).
11. X. Chen, L. Mahadevan, A. Driks, and O. Sahin, *Nat. Nanotechnol.* 9, 137 (2014).
12. L. Sepunaru, I. Tsimberov, L. Forolov, C. Carmeli, I. Carmeli, and Y. Rosenwaks, *Nano Lett.* 9, 2751 (2009).
13. D. Gerster, J. Reichert, H. Bi, J.V. Barth, S.M. Kaniber, A.W. Holleitner, I. Visoly-Fisher, S. Sergani, and I. Carmeli, *Nat. Nanotechnol.* 7, 673 (2012).
14. K.K. Sadasivuni, D. Ponnamma, H.-U. Ko, H.C. Kim, L. Zhai, and J. Kim, *Sens. Actuators, B* 233, 633 (2016).
15. T.-U. Kim, M.-G. Gang, J.-A. Kim, J.-H. Moon, D.-G. Kim, S.-H. Kim, H.-C. Ki, J.-h. Choi, and J.-H. Kim, *Electron. Mater. Lett.* 12, 224 (2016).
16. D. Ponnamma, Q. Guo, I. Krupa, M.A.S.A. Al-Maadeed, K.T. Varughese, S. Thomas, and K.K. Sadasivuni, *Phys. Chem. Chem. Phys.* 17, 3954 (2016).
17. N. Iftimie, E. Rezlescu, P.D. Popa, and N. Rezlescu, *J. Optoelectron. Adv. Mater.* 8, 101 (2006).
18. A. Sutka and G. Mezinskis, *Front Mater. Sci.* 6, 128 (2012).
19. K.V. Rao and C.S. Sunandana, *Synth. React. Inorg. Met-Org Nano-Metal Chem* 38, 173 (2008).
20. M.M.A. Bradford, *Anal. Biochem.* 72, 248 (1976).
21. A. Chowdhuri, V. Guptaa, and K. Sreenivas, *Sens. Actuators, B* 93, 572 (2003).
22. S.K. Kumar, M. Castro, A. Saiter, L. Delbreilh, J.F. Feller, S. Thomas, and Y. Grohens, *Mater. Let.* 96, 109 (2013).
23. K.V. Rao and C.S. Sunandana, *J. Phys. Chem. Solids* 69, 87 (2008).
24. K.V. Rao and C.S. Sunandana, *Solid State Commun.* 148, 32 (2008).
25. A.A.M. Farag, M. Cavas, F. Yakuphanoglu, and F.M. Amanullah, *J. Alloys Compd.* 509, 7900 (2011).
26. D. Rathore, R. Kurchania, and R.K. Pandey, *Sens. Actuators, A* 199, 236 (2013).
27. V.N. Mishra and R.P. Agarwal, *Microelectron. J.* 29, 861 (1998).
28. Y.H. Kim, H. Kawamura, and M. Nawata, *J. Mater. Sci.* 32, 1665 (1997).
29. D.S. Dhawale, D.P. Dubal, A.M. More, T.P. Gujar, and C.D. Lokhande, *Sens. Actuators, B* 147, 488–494 (2010).
30. H.W. Shim, Y.H. Jin, S.D. Seo, S.H. Lee, and D. Wan, *ACS Nano* 5, 443 (2011).